

An Empirical Indoor Path Loss Model For Ultra-Wideband Channels

Saeed S. Ghassemzadeh, Larry J. Greenstein, Aleksandar Kavčić, Thorvardur Sveinsson, Vahid Tarokh

Abstract— We present a statistical model for the path loss of ultra-wideband (UWB) channels in indoor environments. In contrast to our previously reported measurements, the data reported here are for a bandwidth of 6 GHz rather than 1.25 GHz; they encompass commercial buildings in addition to single-family homes (20 of each); and local spatial averaging is included. As before, the center frequency is 5.0 GHz. Separate models are given for commercial and residential environments and within each category, for line-of-sight (LOS) and non-line-of-sight (NLS) paths. All four models have the same mathematical structure, differing only in their numerical parameters. The two new models (LOS and NLS) for residences closely match those derived from the previous measurements, thus affirming the stability of our path loss modeling. We find, also, that the path loss statistics for the two categories of buildings are quite similar.

Index Terms— Path Loss, Signal Propagation, UWB.

I. INTRODUCTION

Interest in commercial usage of Ultra-Wideband (UWB) communication systems has increased dramatically since the Federal Communication Commission (FCC) approved UWB transmission from 3.1-10.6GHz [1]. UWB technology is based on transmission of radar like signals, with its origin in military applications and short-range radar for locating and tracking. Following the approval of UWB for commercial usage, it is being considered as the physical layer for a new indoor wireless personal area networks (WPAN) standard [2]. The working environment of such networks would be indoor residential and commercial buildings. The propagation channel for UWB signals in such environments is the main focus of this paper.

Indoor signal propagation has been extensively studied over the past two decades, e.g., [3]-[6], although indoor measurements over very wide bandwidths are more recent, e.g., [7]-[12]. Here, we report on the large-scale propagation properties of a UWB channel in both residential and commercial indoor environments. Specifically, we construct a

statistical model for the path loss in the environments of interest and conduct simulations confirming its goodness.

The organization of the paper is as follows: Section II covers the implementation of the measurements. Section III gives the basic path loss formula and describes the data reductions. Section IV presents the key findings. Finally, Section V gives the statistical path loss model and the results of our model simulations.

II. MEASUREMENT EQUIPMENT AND DATABASE

A. Equipment and Measurement Parameters

We use a vector network analyzer (e.g., PNA 8538A) to transmit 1601 continuous wave tones uniformly distributed from 2-8 GHz, with a frequency separation of 3.75MHz. This frequency resolution allows us to capture multipaths with maximum excess delay of 266ns. The 6-GHz wide bandwidth gives a time resolution of 166.7ps.

The hardware setup of the experiment is as follows (See Fig. 1): The output port of the PNA is connected to a 30-dB gain power amplifier (PA). The output power of the PA is returned to the reference port of the PNA to compensate for impedance mismatching between the PNA and PA. The boosted power is also connected to a variable attenuator followed by a conical monopole, 11-GHz wide antenna with linear polarization. We use a conical monopole antenna radiating omni-directionally in the azimuth plane, with 0-dBi gain in the range 1-12 GHz. We were able to remove the antenna effects by calibrating the measurement equipment in an anechoic chamber.

A similar antenna receives the signal from the PNA and drives it through a low-noise amplifier (LNA) with a 34dB gain followed by a 45 m long doubly-shielded ultra-low loss coax cable. The output of this cable is then amplified one last

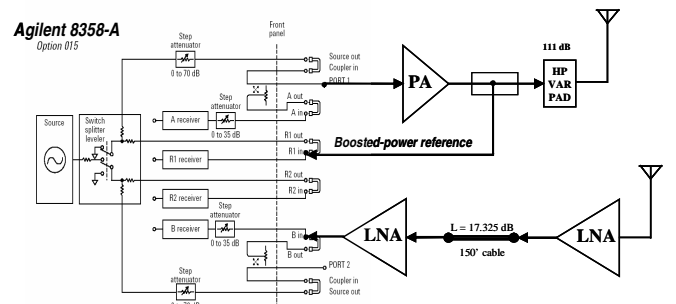


Fig. 1. Measurement transceiver configuration

This material is based upon research supported in part by the National Science Foundation under grant no. CCR-0118701 and the Alan T. Waterman award, grant No. CCR-0139398. Any opinions, findings and conclusions or recommendation expressed in this publication are those of the authors and do not necessarily reflect the views of the National Science Foundation.

S.S. Ghassemzadeh (saeedg@research.att.com, corresponding author) is with AT&T Labs-Research, Florham Park, NJ, USA.

L.J. Greenstein is with WINLAB-Rutgers University, Piscataway, NJ, USA.

A. Kavčić, T. Sveinsson and V. Tarokh are with Division of Engineering and Applied Sciences, Harvard University, Cambridge MA, USA

time by a 41-dB gain LNA before it is received at the input of the same PNA for actual measurement. The measured complex frequency response is stored on a computer hard drive via a GPIB cable controlled by Agilent-VEE programs.

This set-up was properly calibrated in an anechoic chamber to compensate for the effects of impedance mismatching of the antennas with the front-end of the transceiver. The calibration data is also saved for post-processing and reduction of data.

B. Collected Database

The time-invariant nature of the indoor UWB channel has been shown in [10]. Hence, we measured only a single time-snapshot of the channel at each point in space. We captured the small-scale spatial variations of signal power by performing spatial measurements around each location, allowing us to construct the local spatial average of channel gain.

We measured 20 commercial buildings and 20 residences in the greater Boston area and in New Jersey. In each building, we selected around 30 locations, with transmitter-receiver (T-R) separation, d , ranging from 0.8 m to 10.5 m for both line-of-sight (LOS) and non-line-of-sight (NLS) paths. We refer to these points as local points. Around each local point, we performed 25 spatial measurements on a fixed grid. This is illustrated in Fig. 2. We refer to a single point on the grid as a spatial point. The distance between spatial points on the grid was 50 mm. We performed all the measurements with transmitting and receiving antennas in the same horizontal plane; the height of the antennas was 1.8 m.

III. PATH LOSS FORMULA AND DATA REDUCTIONS

A. Path Loss Formula

We define path loss as the dB reduction in power from the transmitter to the receiver location, where the received power is spatially averaged around the location. Specifically, it is averaged over an area whose radius is several wavelengths, with the wavelength being that at the center frequency of the transmission. A general path loss formula that incorporates reflection, diffraction and scattering for both LOS and NLS paths can be stated. It has the well-known form

$$PL(d) = PL_0 + 10 \cdot \gamma \cdot \log_{10}(d/d_0) + S \quad (1)$$

where PL_0 is the point at the reference distance d_0 and γ is the slope of the average increase in path loss with dB-distance. The spatial variation S denotes a zero-mean Gaussian random variable with standard deviation, σ . It can thus be written as

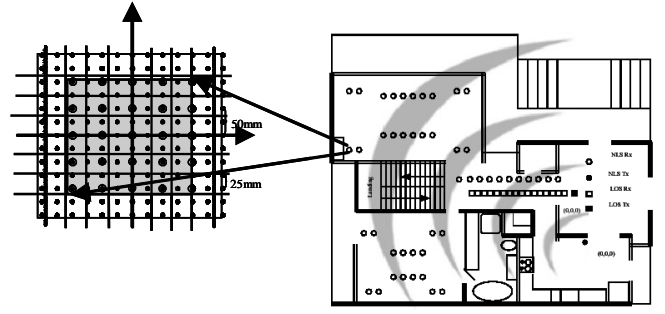


Fig. 2. Illustration of the spatial measurement set-up in a typical building

$S = y\sigma$, where y is a zero-mean, unit-variance Gaussian random variable. The spatial variation of S is usually referred to as *shadowing*, and it captures the path loss deviation from its median value.

B. Data Reductions

After the removal of stored calibration data, for each local point, the database consists of 25 channel complex frequency responses, $H_k(f_i)$. Here, the index k denotes one of the 25 grid positions and the f_i are 1601 discrete frequencies ranging from 2–8 GHz (i.e., $1 \leq k \leq 25$ and $0 \leq i \leq 1600$). We define the spatial *path loss* (in dB) at grid position k and T-R separation d as

$$PL_{sp}^k(d) = -10 \cdot \log_{10} \left(\frac{1}{1601} \sum_{i=0}^{1600} |H_k(d, f_i)|^2 \right). \quad (2)$$

Note that the spatial path loss is relatively insensitive to frequency and therefore we represent it as an average over all frequencies. Since the database consists of measurements from 25 spatial points around each local point, we compute the local path loss by averaging the corresponding set of spatial path losses. Specifically, we perform the linear average

$$PL(d) = 10 \cdot \log_{10} \left(\frac{1}{25} \sum_{k=1}^{25} 10^{\frac{PL_{sp}^k(d)}{10}} \right). \quad (3)$$

From each measured frequency response, we find the spatial path loss from (2) and the corresponding local path loss from (3). For the remainder of this paper, we work with the latter and refer to it simply as path loss.

IV. KEY FINDINGS

We separate our findings into commercial and residential buildings, as well as LOS and NLS paths. For each of the four measured categories, we study the path loss by either pooling data over all buildings or by studying each building separately. Since the center frequency of our measurements is 5 GHz, we expect the path loss values taken from the new homes to be comparable with those of our previous measurements [10]. Recall that the previous measurements were taken in 23 homes over a 1.25-GHz wide frequency band, centered at 5 GHz. The T-R separation of local points ranged from 1 to 15 meters. The path loss values were computed by the same technique as in (2). Later we will increase the statistical fidelity of our database in residential environments by appending the two large data bases. This will result in a combined database of more than 2000 local path loss points spread uniformly inside

Table I. The path loss parameters over all buildings

Environment	PL_0	γ	σ
LOS Commercial	43.7	2.07	2.3
NLS Commercial	47.3	2.95	4.1
LOS Residential	45.9	2.01	3.2
NLS Residential	50.3	3.12	3.8

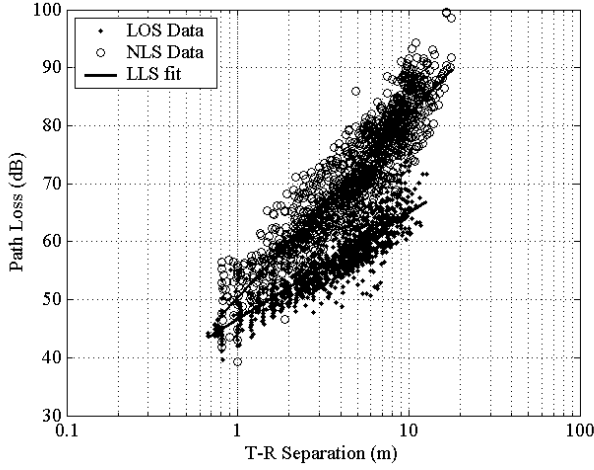


Fig. 3. Path loss vs. T-R separation in residential environments

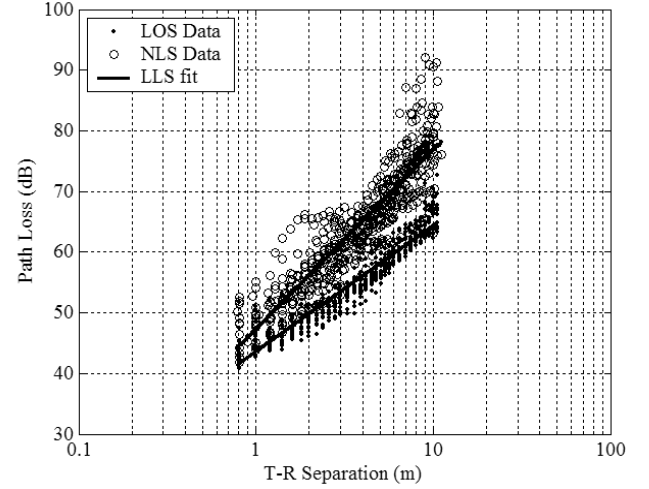


Fig. 4. Path loss vs. T-R separation in commercial environments

43 homes.

A. Path Loss over All Buildings in Each Building

Initially, we pool path loss values (computed from the new set of measurements only) over all buildings within each of the four categories, and we study their statistics. Using the linear least squares (LLS) method, we fit (1) to the scatter-plots of path loss PL and T-R separation d (with $d_0 = 1\text{m}$) and compute PL_0 , γ and σ . Table I summarizes the parameter values for all new measurements. In comparing the results for homes with those reported in [10] and [11], we find that the path loss parameters are very similar. This justifies our later pooling of the new and previous residential data bases.

B. Path Loss Parameter Variations Over Buildings

Differences in building materials, structures and age of buildings cause buildings to exhibit different propagation behaviors. As a result, we expect the slope γ and the standard deviation of shadowing, σ , to vary among buildings. In fact, in [10], we showed how a statistical path loss model can be created by taking γ and σ as random variables over buildings while keeping PL_0 fixed. This follows a similar approach used for path loss modeling in large outdoor cells [13]. We do the same within this work, namely, we fix PL_0 at the mean taken over all buildings and study the statistics over the pool of extracted γ and σ .

Table II summarizes the mean and standard deviation of γ

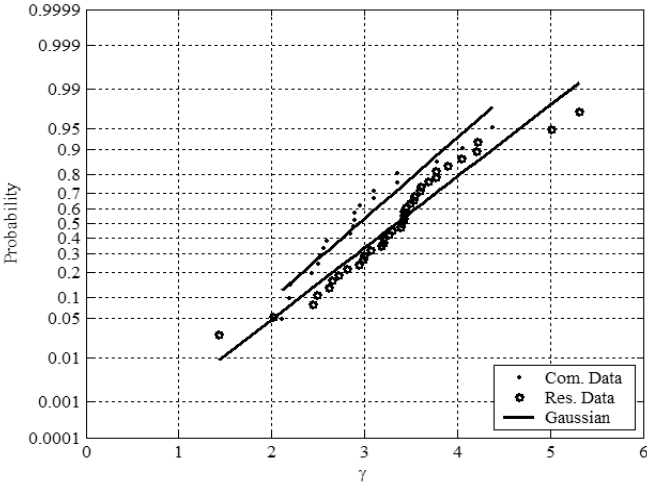


Fig. 5. The distributions of path loss exponent for commercial and residential buildings on NLS paths

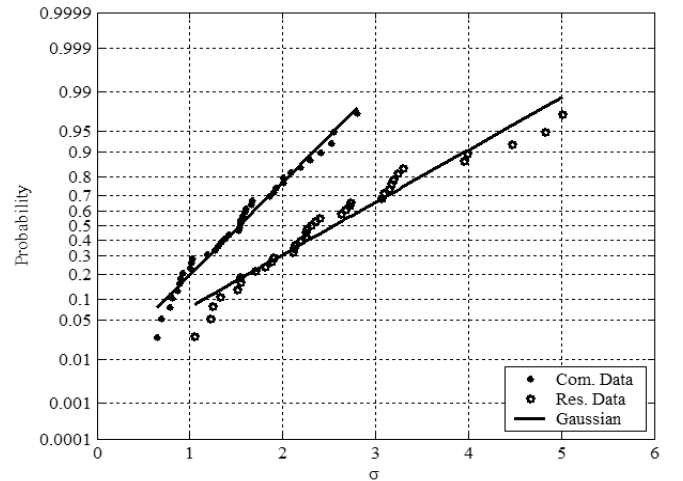


Fig. 6. The distributions of standard deviation of shadowing for commercial and residential buildings on NLS paths

Figure 3 shows scatter plots for LOS and NLS paths in homes (new and previous data pooled), while Fig. 4 shows corresponding scatter plots for commercial buildings (new data only). We see that the main difference between building types is a somewhat higher NLS path loss, on average, in homes. Further measurements in commercial buildings would help test the stability of these results.

and σ for all environments, along with their corresponding values for PL_0 (Here, we denote the mean and standard deviation of γ as μ_γ and σ_γ , respectively, and the mean and standard deviation of σ as μ_σ and σ_σ). Figures 5 and 6 show cumulative distribution functions of γ and σ , respectively, in commercial and residential buildings on NLS paths. We

observe similar behavior on LOS paths. We find the correlation coefficient between γ and σ in homes to be fairly low (-0.08 and -0.19 for LOS and NLS paths, respectively). Corresponding correlation coefficients for commercial buildings are 0.19 and 0.41 on LOS and NLS paths, respectively.

Finally, we examine the statistics of S , the dB deviation from the median path loss. Fig. 7 shows two CDFs for NLS paths, one for all residences and one for all commercial buildings. Similar results are obtained for LOS paths. For residences in particular, we see excellent agreement with the log-normal assumption for shadow fading.

V. THE PATH LOSS MODEL AND SIMULATIONS

A. The Path Loss Model

We define a statistical path loss model based on (1), with a fixed intercept point PL_0 , but treating γ and σ as random variables over buildings. Based on Figs. 5 and 6, we can approximate γ and σ as Gaussian variables.

We could also incorporate the correlation coefficients between them into the model (e.g., using Cholesky factorization [14]). However, our simulation results show little-to-no impact and thus, little justification for including an extra model parameter. Therefore, for simplicity of the model, we assume independence between the parameters γ and σ .

The Gaussian distribution is completely defined by its first and second moments, allowing us to write

$$\begin{aligned}\gamma &= \mu_\gamma + \sigma_\gamma \cdot x_1 \\ \sigma &= \mu_\sigma + \sigma_\sigma \cdot x_2\end{aligned}\quad (4)$$

where x_1 and x_2 are iid zero-mean, unit-variance Gaussian random variables which vary from building to building. Then we define the complete statistical path loss model as

$$PL(d) = \underbrace{PL_0 + 10 \cdot \mu_\gamma \cdot \log_{10}(d)}_{\text{Median path loss}} + \underbrace{10 \cdot \sigma_\gamma \cdot x_1 \cdot \log_{10}(d) + y \cdot \mu_\sigma + y \cdot x_2 \cdot \sigma_\sigma}_{\text{Deviation from median path loss}}. \quad (5)$$

The deviation from the average path loss is a combination of effects from the two zero-mean, unit-variance Gaussian random variables x_1 and x_2 and the zero-mean, unit-variance Gaussian random spatial variable y . We should emphasize that the random variables x_1 , x_2 and y should be truncated so as to not take on values outside the range computed from data.

B. Simulations

We simulated the path loss model (5) and compared it to that obtained from measurements. For each environment, we generated 20 realizations of x_1 and x_2 , representing the number of measured buildings. We also generated 93 pairs of d and y for each pair of x_1 and x_2 , representing the distance and shadowing at each location per building.

In Figs. 8 and 9, we show the comparison between the simulated results and measured scatter plots of NLS path loss in residential and commercial buildings, respectively. We

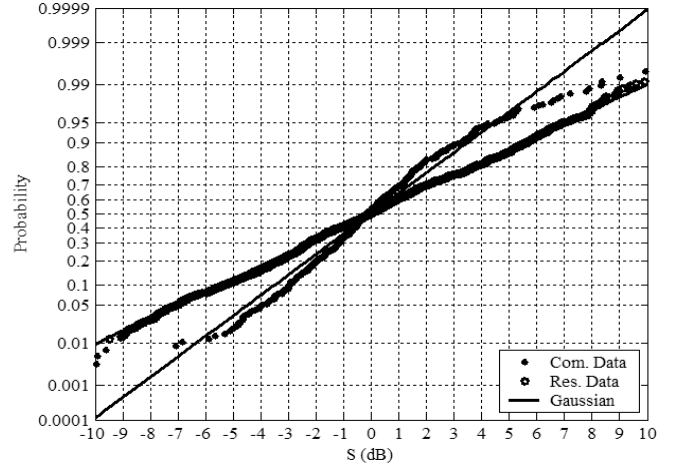


Fig. 7. The shadowing distributions for residential and commercial buildings on NLS paths

observed similar results for LOS paths. Parameters from the simulations are summarized in Table III and can be compared with those in Table I. The discrepancies are minor. Moreover, recall that the residential data used to obtain Table I were from new measurements only, while the data used to obtain Table III included this database together with the one reported in [10]. This, we find, is the cause of most of the differences between these tables. We conclude that our model succeeds in generating path loss statistics very close to those of the database.

Table II. Parameter values in path loss model

Environment	PL_0	μ_γ	σ_γ	μ_σ	σ_σ
LOS Commercial	43.7	2.04	0.30	1.2	0.6
NLS Commercial	47.3	2.94	0.61	2.4	1.3
LOS Residential	47.2	1.82	0.39	1.5	0.6
NLS Residential	50.4	3.34	0.73	2.6	0.9

Table III. Path loss parameters from simulation

Environment	PL_0	γ	σ
LOS Commercial	43.7	2.06	2.6
NLS Commercial	46.8	3.03	3.9
LOS Residential	47.2	1.84	3.0
NLS Residential	50.3	3.29	4.4

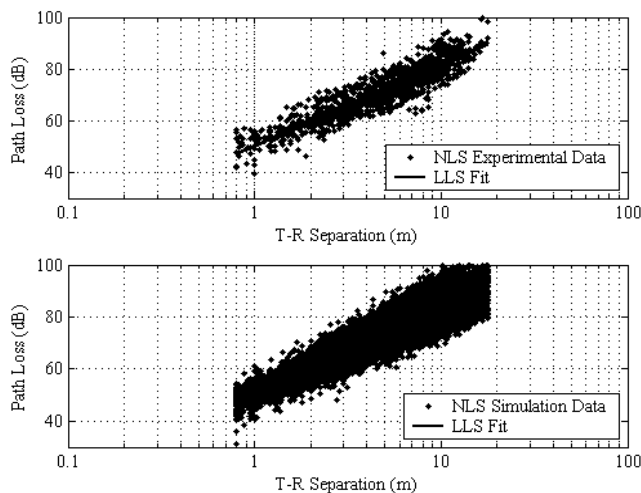


Fig. 8. Path loss: Simulated vs. measured in residential buildings.

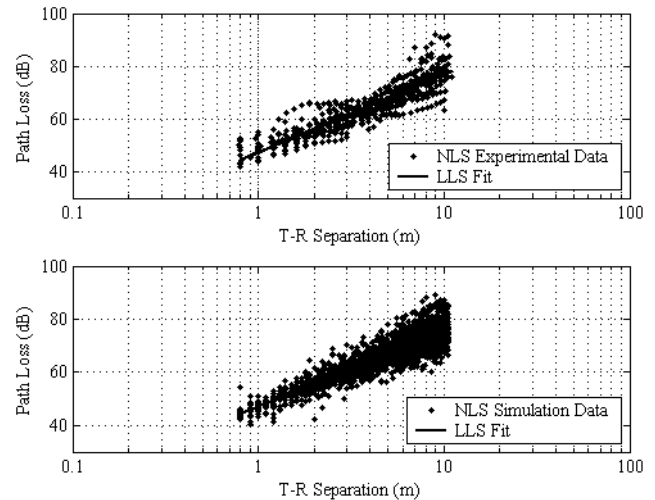


Fig. 9. Path loss: Simulated vs. measured in commercial buildings.

VI. CONCLUSIONS

We have reported path loss findings from extensive measurements of a wireless UWB channel in 20 commercial buildings and 43 homes. We used a previously proposed statistical path loss model as a basis for modeling the path loss of the channel and confirmed its goodness. Moreover, the agreement of the current model for residences with those reported in [10] and [11] is excellent. The earlier model was based on measurements over 1.25 GHz, without spatial averaging, and for a different population of homes (or some of the same homes but different paths). The repeatability of the model, combined with its relative simplicity, makes it both reliable and useful for characterizing indoor path loss. Further measurements in commercial buildings would help to establish model stability for that category.

ACKNOWLEDGEMENT

The authors thank Alexander Hiamovich and Haim Grebel for use of their anechoic chamber at the New Jersey Institute of Technology; Chris Rice of AT&T Labs-Research, for valuable comments and suggestions on the hardware set-up; and lastly but not least, all the homeowners from AT&T Labs and Harvard University who graciously allowed us to invade their premises with our measurements.

References

- [1] FCC Document 00-163: Revision of Part 15 of the Commission's Rules Regarding Ultra-Wideband Transmission Systems, ET Docket No. 98-153, April 22, 2002.
- [2] IEEE 802.15.3, IEEE standard for wireless personal networks (WPAN), URL: <http://www.ieee802.org/15/pub/TG3a.html>.
- [3] A.A. Saleh, R.A. Valenzuela, "A statistical model for indoor multipath propagation", *IEEE J. Sel. Areas Commun.*, 5:128-137, Feb. 1987.
- [4] S.J. Howard, K. Pahlavan, "Measurement and analysis of the indoor radio channel in the frequency domain", *IEEE Trans. Instrum. Measure.*, 39:751-755, Oct. 1990.
- [5] T.S. Rappaport, S.Y. Seidel, K. Takamizawa, "Statistical channel impulse response models for factory and open plan building radio communication system design", *IEEE Trans. on Commun.*, 39:794-806, May 1991.
- [6] H. Hashemi, "The indoor propagation channel", *Proc. of the IEEE*, 81:943-968, July, 1993.
- [7] D. Cassioli, M.Z. Win and A. Molisch, "The ultra-wide bandwidth indoor channel: from statistical model to simulations", *IEEE J. Sel. Areas Commun.*, 20: pp 1247-1257, Aug. 2002.
- [8] J. Foerster, "Channel Modeling Sub-committee Report Final", IEEE P802.15-02/368r5-SG3a.
- [9] R. Addler, D. Cheung, E. Green, M. Ho, Q. Li, C. Prettie, L. Rusch, K. Tinsley, "UWB channel measurements for the home environment", *UWB Intel Forum*, Oregon, 2001.
- [10] S.S. Ghassemzadeh, et al. "A statistical path loss model for in-home UWB channels", *Proc. IEEE conf. on Ultra Wideband Systems and Technologies*, pp: 59-64, May 2002.
- [11] ———, "Measurement and modeling of an ultra-wideband indoor channel", *IEEE Trans. on Commun.*, Dec. 2003.
- [12] S.S. Ghassemzadeh, L.J. Greenstein, A. Kavčić, T. Sveinsson, V. Tarokh, "UWB indoor delay profile model for residential and commercial buildings", in *Proc. IEEE VTC-Fall 2003*.
- [13] V. Erceg, et al., "An empirically based path loss model for wireless channels in suburban environments", *IEEE J. Select. Areas Commun.*, 17:1205-1211, July 1999.
- [14] C.D. Meyer. "Matrix analysis and applied linear algebra". 2000 SIAM.